

Accretionary lapilli: what's holding them together?

Paul M. Adams,¹ David K. Lynch² and David C. Buesch³

¹Thule Scientific, P.O. Box 953, Topanga, CA 90290 USA, paul.m.adams@aero.org; ²U.S. Geological Survey, 525 South Wilson Ave., Pasadena, CA 91106-3212 USA; ³U.S. Geological Survey, 345 Middlefield Road, Menlo Park, CA 94025 USA

ABSTRACT: Accretionary lapilli from Tagus cone, Isla Isabela, Galápagos were analyzed using scanning electron microscope (SEM) and energy-dispersive X-ray spectroscopy (EDS) techniques. Our main findings are (1) the lapilli formed and hardened in a few minutes while still aloft in the dispersing eruption column, (2) palagonite rinds developed first on the basaltic glass clasts, and subsequently crystallized, (3) the crystallization products contain submicron lamellar crystals of a clay (probably smectite) on the surfaces of basaltic glass clasts, and (4) the interlocking of these lamellar clays from adjacent clasts binds and cements them together to form the accretionary lapillus. We argue that palagonite and possibly clay formation occur primarily in the presence of hot water vapor.

1. Introduction

Lapilli (singular lapillus) are pyroclastic particles of any shape with diameters of 2–64 mm that have fallen to the ground after volcanic eruptions. Accretionary lapilli (AL) are small, spheroidal balls of aggregated ash that are sometimes formed when water meets magma and violently flashes to steam. Most are created during phreatomagmatic eruptions but other types of eruptions involving water can produce them¹⁻⁴. It is also possible that preexisting atmospheric water vapor can provide the necessary moisture. AL can also form in the plume from an asteroid impact^{5,6} and may have been found on Mars⁷. In the California deserts, Ubehebe Crater and at least one of the Salton Buttes were created by phreatomagmatic eruptions^{8,9}, though to date no

AL have been found except in northern and central California¹.

Formation and growth of AL occurs in the eruption column and dispersing ash cloud. Development may proceed along several different paths, but all seem to involve aggregation¹⁰ of ash particles in the presence of water in any of its three phases. Electrostatic attraction is also thought to promote their formation. Different parts of the ash eruption column may have different grain sizes and particle morphology and so each lapillus grows by adding distinct concentric layers. Eventually the AL fall to the ground, and thus are somewhat analogous to hailstones. Depending on formation conditions, lapilli can vary between muddy rain, mud balls or hard spheres. The cementation process is not well understood.



Figure 1. Location map of Tagus cone, Isabela Island, Galápagos

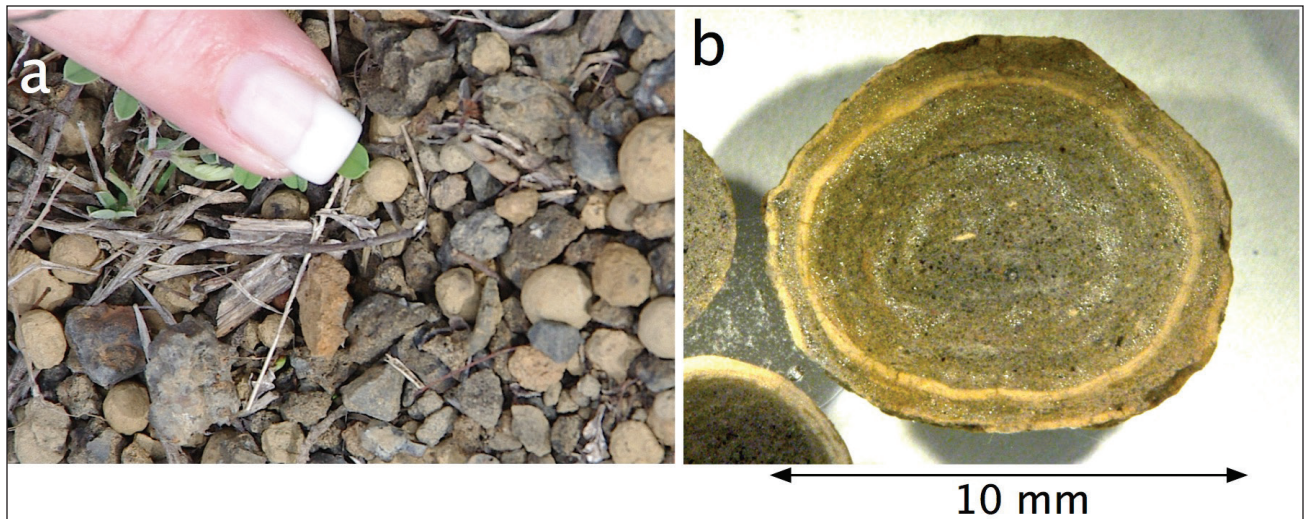


Figure 2. (a) Lapilli at the collection site. (b) Cross section of typical accretionary lapillus.

Accretionary lapilli are found in many parts of the world including the Galápagos Islands. Several dozen AL were collected on 12 Feb 2013 from a small area on the north flank of Tagus cone, a cone on the coastline (possibly a littoral cone) on Darwin Volcano, Isabela Island (Figure 1). The age of the cone is not known, but geomorphic features appear fairly young and is only slightly rilled. The southern section has been breached and the ocean side slopes have been eroded by wave action. The islands are on the Nazca Plate near the Galápagos Triple Junction and are composed primarily of mid-ocean-ridge basalts (MORB). Darwin volcano is an active shield that last erupted in 1813¹¹. Palagonitic soil and tuff are common in the area because palagonite is a common and an almost immediate alteration product when water interacts with basaltic glass¹². The term “palagonite” has been used as a mineral assemblage (a relatively homogeneous, amorphous to poorly crystalline replacement product of basaltic glass) or to mean different sedimentary and alteration facies in tuffaceous rocks. Here we use it to mean the hydrothermally altered or hydrated but amorphous to poorly crystallized material derived from glassy basalt. Palagonite is typically yellow-brown in color due to ferric oxide Fe_2O_3 , (rust), i.e., the same color as the AL reported here. In this paper we report detailed analyses of the AL with the goal of understanding the cementation process.

2. Macroscopic properties

As encountered on the ground, accretionary lapilli are loose and numerous with hundreds per square meter. Also present are abundant lithic lapilli. Nearby there are exposures of lapilli tuff that contained AL, and it

is not clear whether these deposits might be the source bed for the sampled AL, but none of the AL sampled have what appears to be attached matrix from a host rock. The AL are well indurated, i.e., too hard to crush between the fingers. AL have smooth surfaces, are round to mildly oblate, range between 5 and 15 mm in diameter and are tan in color (Figure 2). They show little or no surface color variations. There appears to be no differences between the tops and bottoms, as there might be if weathered or bleached by the sun. Mass and volume measurements of three lapilli show porosities ranging between 40% and 60%. When soaked in water they do not disaggregate. Immersion in hydrochloric acid produces no reaction.

Seven AL were cut open with a diamond saw, vacuum impregnated with epoxy and polished to reveal the internal structure. AL were cut, as close as possible, to expose the center of the AL, and none had a central lithic clast core or “seed” as would an armored lapilli. All have the characteristic concentric layering, and different layers have different colors and textures with significant porosity ranges among the layers.

3. Microscopic analyses

Samples were examined in a JEOL model 7600F field emission scanning electron microscope (SEM) equipped with an Oxford X-Max energy dispersive spectrometer (EDS). An accelerating voltage of 2KV was used for high resolution imaging of non-carbon coated samples while 15 KV was used for EDS analyses of carbon-coated samples. When EDS analysis for carbon was required, uncoated samples were examined in a JEOL model 6460LV variable pressure SEM.

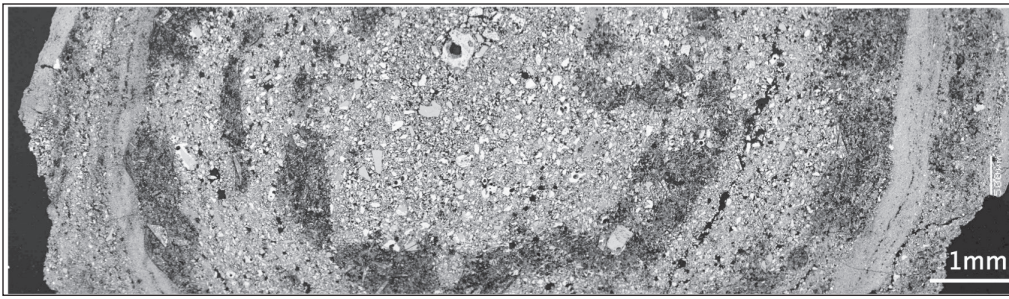


Figure 3. Backscatter SEM image of lapillus #1 polished cross section. Layering is mostly concentric, but thickness of layers is not constant, and some layers are not traceable around the entire lapillus.

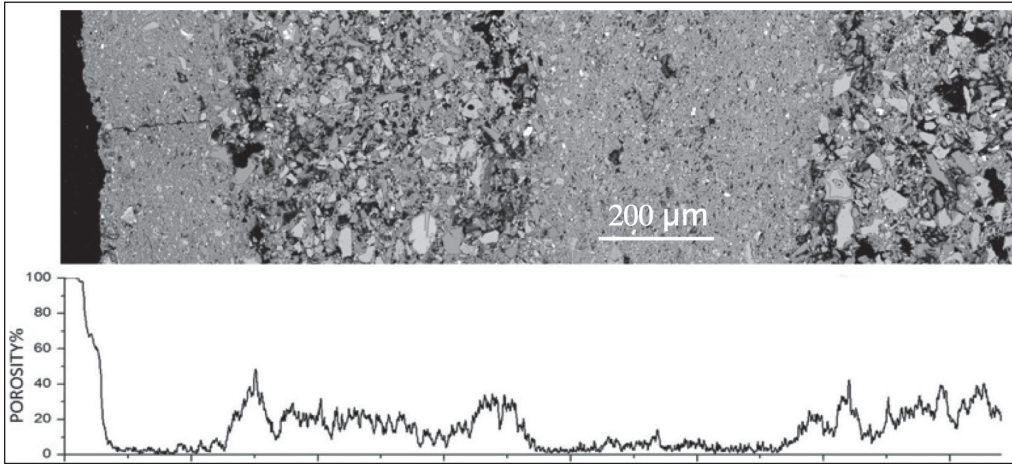


Figure 4a. Backscatter SEM image of lapillus #2 polished cross section with porosity profile calculated from binary image. The radius of lapillus #2 is 7 mm. Average largest dimension of particles in center dense band and rim is 7 μm.

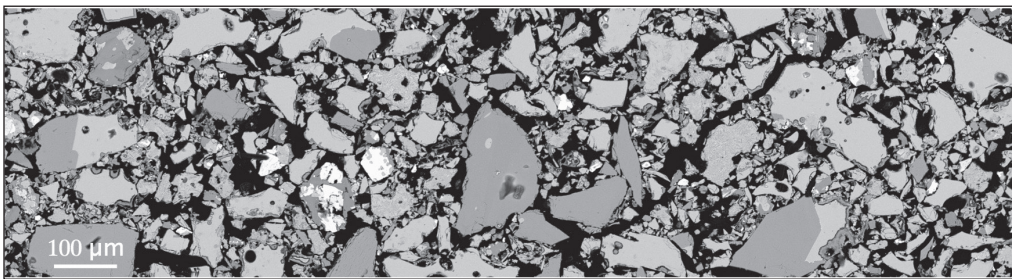


Figure 4b. Backscatter SEM image of center of lapillus #2. Porosity is about 35%. Average largest dimension of particles is 35 μm.

4. SEM imagery

In the scanning electron microscope (SEM), polished sections reveal a wealth of heterogeneous morphology on all scales (Figure 3). The main layering is evident in both packing density and clast size, and these textures are sometimes correlated; in general, clasts are larger near the center of the lapilli and become smaller toward the surface but with considerable variation. All lapilli have exterior layers composed of small closely spaced particles. Center-to-edge SEM mosaics were thresholded with Image-J image analysis software to produce binary images where voids are black and solids are white. The

Image-J box tool was used to produce a line profile where the average gray level can be correlated with the percent porosity (0 = 100% porosity, 255 = 0% porosity). An example is given in Figure 4a.

The grain components include rock fragments, crystals (plagioclase, pyroxene, and olivine), glass with devitrified rinds and voids. In backscatter electron images the main components of glass, crystals (plagioclase), devitrified rinds (or grains) and voids can be distinguished by gray level (in decreasing order). Gray level thresholding in the SEM/EDS software was used to estimate the relative abundances. In several lapilli the proportions of glass,

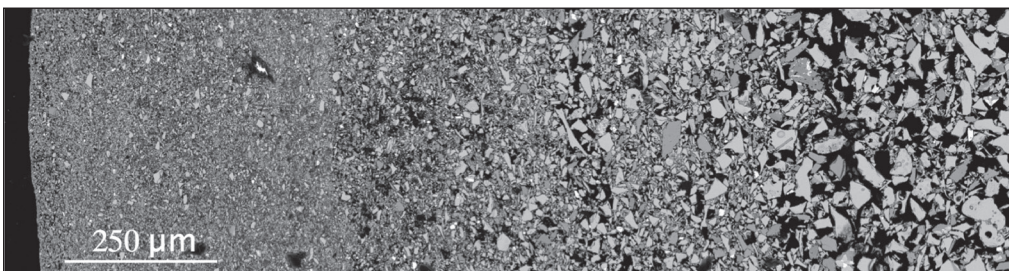


Figure 5. Backscatter SEM image of lapillus #3 (5.5 mm radius) polished cross section. Note the gradual decrease in particle size toward the surface (left edge of image).

Figure 6. Backscatter SEM images of lapillus #1 polished cross section. Left: Light gray glass shards (G) have concave surfaces, voids and thin palagonized rinds (R). Medium gray grains are plagioclase or pyroxene (P). White grains are Fe-Ti oxides. Right: close up of highly palagonized glass shard.

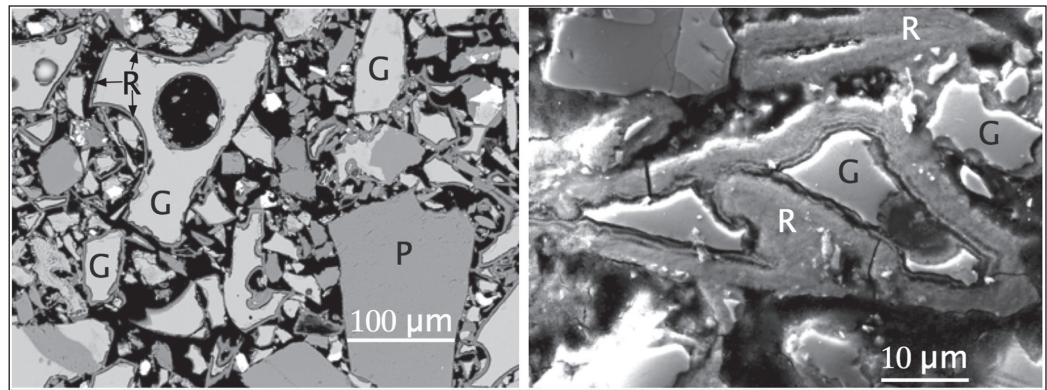
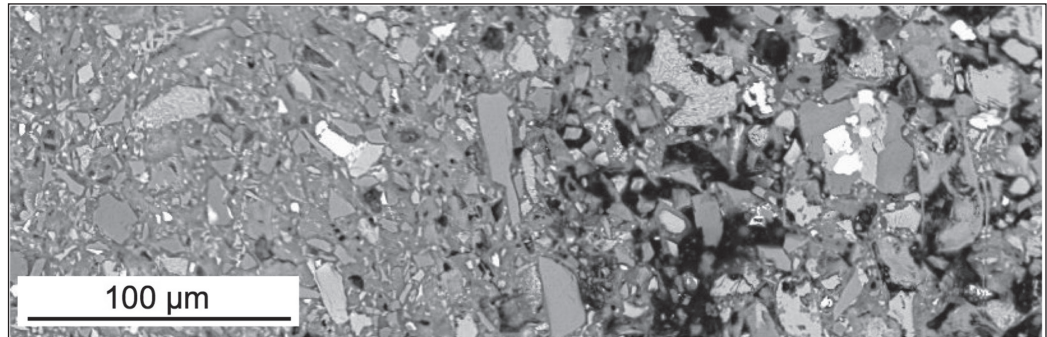


Figure 7. Backscatter SEM image of lapillus #2 polished cross section (upper left in Figure 4a). Most of the glass on the left has been palagonized. Remaining clasts are predominantly plagioclase.



crystals and devitrified material are approximately equal. In lapillus #3, however, there is a marked difference in the degree of devitrification between the core (17%) and rim (59%), and this correlates with decrease in porosity from the core (31%) to the rim (15%), (Figure 5).

Most glass shards have concave surfaces, indicating that they are parts of bubble walls. Indeed, vesicles (“bubbles”) are commonly preserved (Figure 6). A large fraction of the glassy clasts shows altered palagonite rinds paralleling the surfaces, but crystals of plagioclase and pyroxene lack such rinds. The rinds are darker in the SEM imagery, the result of a lower mass density compared their parent clasts. Lower mass density can occur in two ways: 1) hydration during alteration, 2) the development of nanovoids. Palagonite is an alteration product of basaltic glass and is widely observed when basalt is exposed to water¹³⁻¹⁶. The rinds are fairly uniform in thickness, about 2 µm, and many are slightly separated from the clasts and show internal layering.

Accumulations of very small completely altered glass shards and broken rinds form bands of very low porosity, such as the rims and internal layers of lapilli (Figures 4a, 5). These small rind pieces may represent mechanical spalling from the original host glass grain, then separation and sorting of the rind piece from the glass grain. A close up of one of these dense closely packed layers, which contains only devitrified material and small plagioclase and pyroxene grains (average maximum

dimension 7 µm), is shown on the left in Figure 7. Clasts appear to be arranged randomly, though occasionally there is some evidence of alignment and systematic orientation.

In the laboratory, some lapilli were broken open by crushing. SEM images of the fracture surfaces reveal that breakage was (1) along crystal and glass-shard grain boundaries, (2) rarely across crystal or glassy grains, (3) between glass shards and rinds, and (4) across narrow “bridges” of lamellar material that connect larger grains. The surfaces of the glassy clasts underneath the palagonite rinds are typically etched. All the surfaces of glassy clasts and palagonite rinds have a coating of submicron lamellar or platy crystals (Figure 8). The lamellar coating is absent on plagioclase or pyroxene grains.

5. Chemical composition

Energy Dispersive Spectroscopy (EDS) in the SEM was used to determine the compositions of the individual constituents. Table 1 gives the compositions of typical plagioclase crystals, glass clasts and palagonized rinds. Note that the lamellar coatings on rinds (Figure 8) are too small to be independently analyzed by EDS because the EDS interaction volume is on the order of 1 µm. Figure 9 shows ternary composition diagrams for plagioclase and pyroxene grains from a single representative lapillus. The plagioclase grains do not show

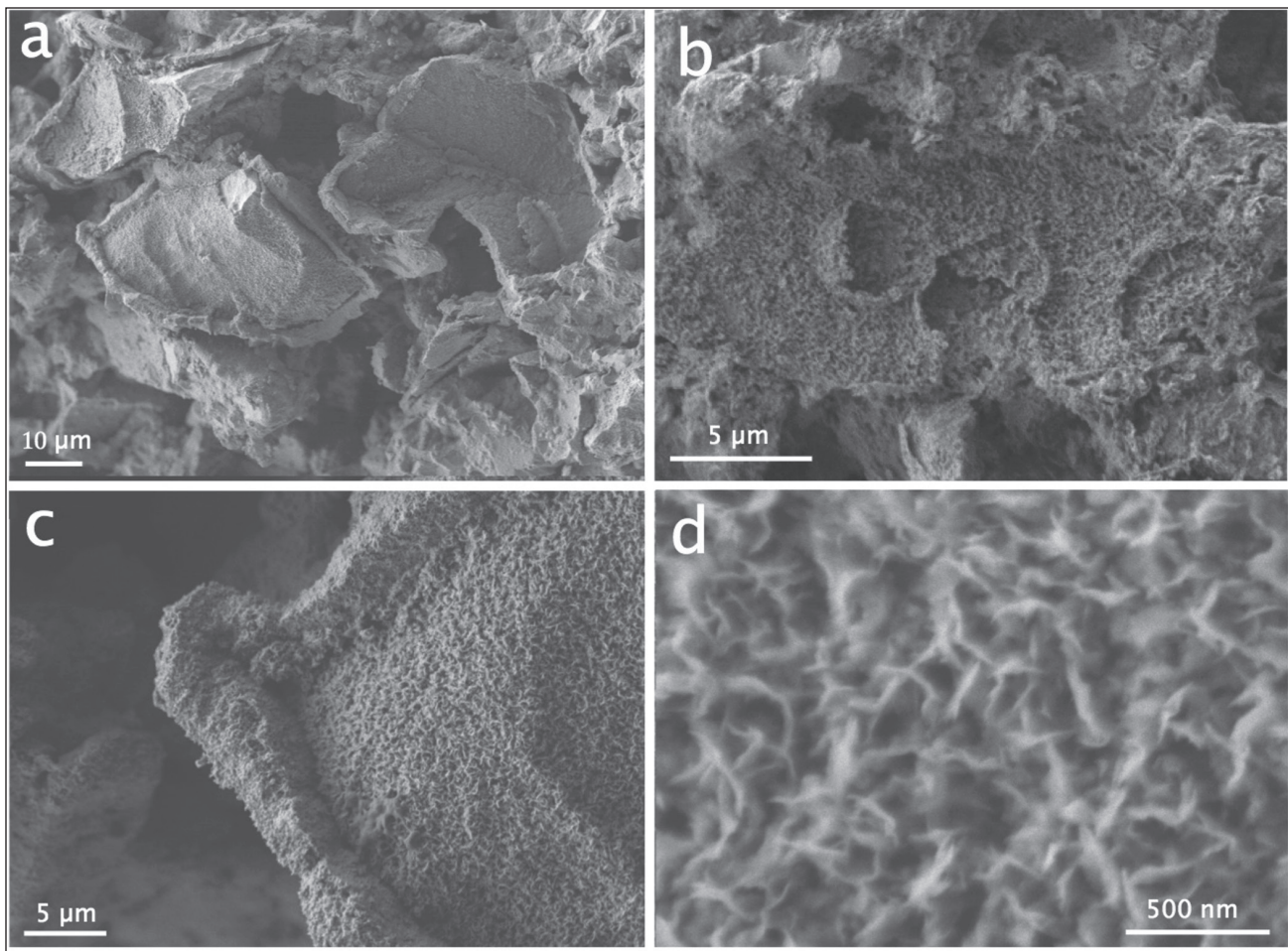


Figure 8. Low voltage SEM image of fractured lapillus surfaces showing submicron lamellar material coating surfaces of glass shards and interior and exterior surfaces of palagonite rinds. (a) Lapillus #1: Glassy clasts with rinds. (b) Lapillus #3: lamellar coating on surface. (C) Lapillus #1: lamellar coating on clast (right) and rind (left). (d) Lapillus #1: Close up of lamellar coating showing interlaced crystals.

significant zoning, based on backscatter SEM images, but do show a bimodal distribution with compositions in both the bytownite and labradorite–andesine fields. Pyroxenes are ferrosilite poor (Fs7–23) augite. These compositions are consistent with mid-ocean-ridge basalts.

The composition of the glass shards is basalt based on Le Bas et al.’s classification in the total-alkali-silica diagram (TAS)¹⁷. The MgO-Na₂O-K₂O ternary diagram (Figure 10) best shows the differences between the glass shards and palagonite rinds. In the rinds, Na₂O is absent with generally minor enrichment in K₂O. There is also a slight increase in CaO in the rinds with respect to Al₂O₃ and SiO₂. The rinds also show significantly low analytical totals (Table 1), a result

of the very fine-grained material taking a poor polish, having moderate porosity, or significant hydration. Normalizing the rind compositions to 100% shows that, in addition to depletion in Na₂O, there are also significant decreases in MgO and CaO coupled with

Table 1. Compositions (wt%) of selected lapilli constituents

	Plagioclase	Plagioclase	Glass	Glass	Rim	Rim
SiO ₂	48.15	59.24	48.25	48.36	36.14(49.87)*	30.82(42.83)
TiO ₂			2.69	2.44	2.88(3.97)	4.80(6.67)
Al ₂ O ₃	33.86	25.88	13.87	14.47	11.90(16.42)	10.98(15.26)
Fe ₂ O ₃	0.72	0.79	11.31	11.24	11.81(16.30)	17.02(23.66)
MnO					1.03(1.42)	
MgO			6.53	6.76	3.12(4.31)	3.27(4.56)
CaO	15.86	6.98	10.26	10.53	4.45(6.14)	3.69(5.13)
Na ₂ O	1.89	7.25	3.00	2.79	0.49(0.64)	
K ₂ O		0.65	0.36	0.58	0.59(0.81)	1.17(1.63)
Total	100.48	100.78	96.26	97.17	72.41(100)	71.74(100)

*values in parentheses are normalized to 100% for better comparison with unaltered glass.

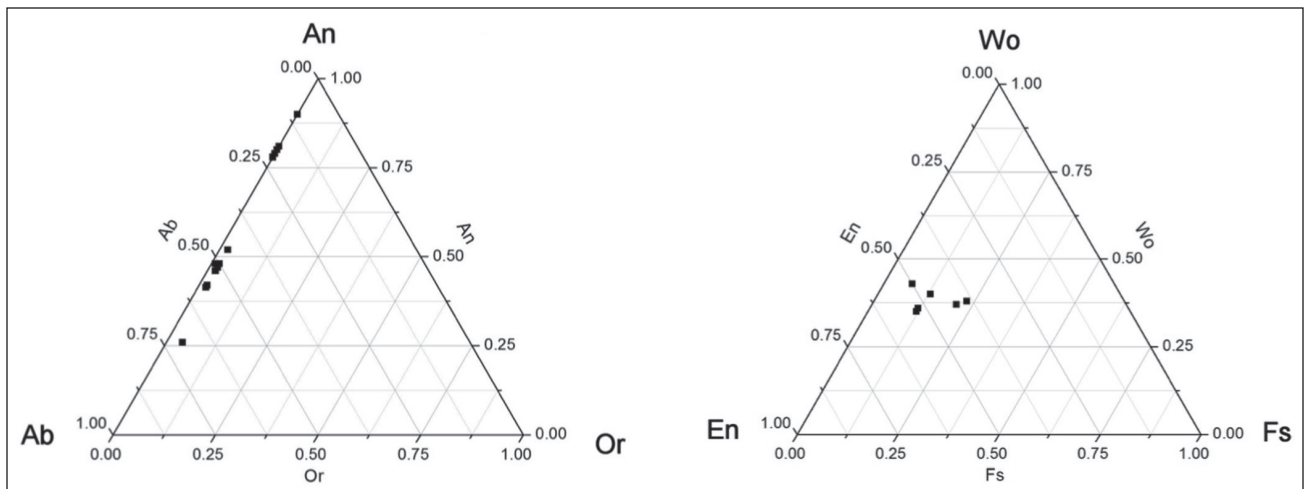


Figure 9. Ternary composition diagrams for plagioclase feldspar and pyroxenes.

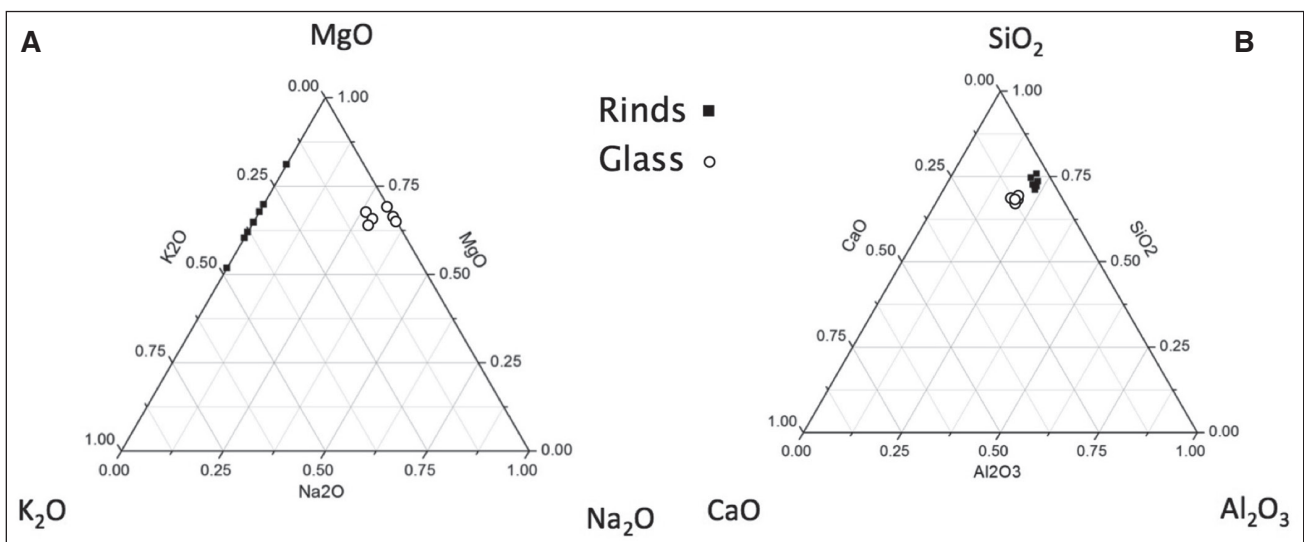


Figure 10. Ternary composition diagrams for glass shards and palagonite rinds.

enhancements in Fe_2O_3 , MnO and TiO_2 . This is consistent with the loss of more mobile species during palagonization¹².

6. Discussion

The eruption that produced the Tagus cone AL was relatively recent because the AL were found loose on the ground, i.e., not covered, and showed no sign of erosion or aging. There is some palagonite lapilli tuff exposed nearby, but it is not clear whether these beds were the source of the collected AL, and the weathering characteristics of these deposits differ from the location of the collected AL. The tan color of the AL is almost certainly due to Fe_2O_3 (rust) and/or the occurrence of palagonite. Indeed, the palagonite tuff exposed near where the AL were found is the same color, varying slightly over the area.

In the Tagus cone AL, glassy clasts are so abundant that they are almost certainly juvenile, i.e., formed by fragmentation and ejection of lava during the eruption. In contrast, a purely phreatic eruptions can eject older, crystallized clasts like those found in the 1790 accretionary (armored) lapilli-bearing ash at Kīlauea^{18,19}.

The complicated layering of grain sizes, and the types and abundances of grains (crystal fragments, glass shards, and rock fragments), indicate that growth of the accretionary lapilli resulted from changing availability of these components in the dynamic environment of an eruption column and distribution plume. In all layers of the lapilli, various amounts of very fine-grained shards occur, some partially coating larger grains or forming bridges between the larger grains. These differences in size, concentration and abundance of grains are consistent with differing amounts of energy and

materials in a vigorously turbulent system as individual cells of air, water vapor, and particles evolve, and where a lapillus is caught up in and transferred to another turbulent cell. Layers that range in thickness around the lapillus, and locally pinch out, might result from the short duration the lapillus traversed a region of one composition (aggradation on the leading side and not the trailing side), or collisions between lapilli that knocked off edges. The rind pieces might have been knocked off their parent glass shard, or spalled during changes in temperature or hydration, and then were mechanically sorted from their parent grain during transfer from region to region. In all the lapilli, the outer surface layer of is very fine grained, and is consistent with the lapilli falling through an overall finer-grained and lower energy environment such as the outer edges of an eruption column or the distribution plume.

The notion that AL are spherical because water drops are spherical and that aggregation took place primarily in the presence of water drops via surface tension seems untenable: rain drops do not reach diameters of 5–15 mm²⁰. Any drop larger than 4–5 mm in diameter will fragment into smaller drops by aerodynamic forces. Spherical accretionary lapilli have been produced in laboratory experiments within a range of 12–45% relative humidity and a wide range in grain size, especially with abundant very fine grains²¹.

Spherical aggregation can occur if a lapillus tumbles while falling through the ash cloud, thereby exposing every surface to the flux of particles. Such aggregation is similar to the formation of hailstones, which are also roughly spherical and show concentric internal layering. Tumbling is the most common form of motion for irregular particles because of the complexity of the inertia tensor. Furthermore, aerodynamic drag and lift on an asymmetric particle will force it into chaotic motion.

If the lapilli were not fully hardened on impact, they might still have remained intact if they fell into a soft ash bed; as would be the case if a previous event had deposited an ash layer. Also, erosion might have removed the ash bed leaving the lapilli on the ground; however, there is no evidence of residual matrix from a host ash bed that is still attached to the AL. If the lapilli were not fully hardened on impact, and they remained intact, it is possible that they would have flattened a bit, become oblate, and formed a flat side where the AL impacted and rested on the ground. This type of shape distortion seems unlikely because it would suggest a correlation between

lapillus diameter and oblateness where the larger lapilli might be more prone to this deformation resulting from size, volume, mass, and low cohesion relations. We saw no correlation between oblateness and diameter.

The AL appear to have formed the shapes and hardened while still aloft, otherwise they would likely have disaggregated on impact. Terminal velocities for AL of the observed mass densities in the 5–15 mm diameter range are 10–20 m/s. They must also have been cool, as there was no evidence that the AL were part of a welded tuff, although there was lapilli tuff in the area. The AL were slightly oblate and few if any were prolate. This is probably the result of spinning as they formed. It could also have been the result of slight flattening on impact, but such events would have produced flat sides and/or possible fractures of the external layers and we have little or no evidence of either.

Previous work on AL has identified basalt chemistry, heat, and water as key elements in AL formation, and some work has proposed involvement of various types of salts being involved in the grain aggradation cementation. A crucial factor in understanding the cement's origin and chemistry is that the cement must have formed and hardened in the few minutes aloft.

Time aloft is difficult to specify with any certainty. Reported time between eruption and ash aggregates arriving on the ground is in the 5–30 minute range for a high-standing, dike-driven eruption column¹⁰. During this time, the component clasts in the eruption column were hot and immersed in dynamic water clouds, so aqueous chemistry would be expected. Phreatic and phreatomagmatic eruptions from littoral cones tend to be much less violent than dike-driven eruptions; therefore, the ejecta would probably have been aloft for less time.

The palagonization rate is strongly temperature dependent²². Assuming 10 minutes aloft, a 2 μm thick palagonite rind would form if the average clast temperature was about 164° C, which is consistent with the expected temperature of a cooling and dispersing eruption column. The palagonization rate, however, is so strongly temperature dependent that the rinds could have formed in a much shorter time if their average temperature was a higher. For example, if they were only aloft for 1 minute, the temperature necessary to produce a 2 μm thick rind would be 245° C, and this is well within the expected range of temperatures in a less violent eruption column.

In the Tagus cone AL, the observed layering of the rinds (micro) and lapilli (macro) can be explained by

variable palagonization rates as the growing lapilli passed through different temperature, moisture and particle size/composition regimes. We assume that palagonization is, at least initially, an ongoing process that begins as soon as hot particles are exposed to water (or water vapor) and proceeds at varying rates depending on temperature and availability of water. Palagonization will not, however, continue indefinitely because the clay forms a moisture-proof, passivation layer, effectively sealing the rinds.

7. What's holding the tagus cone accretionary lapilli together?

Our analyses suggest that the cement binding the AL together was initially palagonite, followed by the ubiquitous lamellar coating (Figure 8) on the exterior of the rinds as seen in the SEM mages of the fracture surfaces. When a heterogeneous solid consisting of strong clasts and relatively weaker cement is broken, cement remains on opposing faces of the fracture (Figure 11). We further argue that the rinds formed before the lamellar coating. Abundant evidence indicates that the chemical evolution of basaltic glass in the presence of water begins with palagonization and is often followed by complete crystallization of the palagonite to smectite¹²⁻¹⁶. High magnification SEM images show that the morphology of the lamellar coating is virtually identical to that of smectite found in many other sources, and the composition of the coating is consistent with the chemical analyses. Since the fracture surfaces show lamellar coatings, we interpret this to mean that the palagonite rinds underwent crystallization and that lamellar smectite on the surfaces of adjacent clasts interlock, acting as cement. Smectite development may have resulted from dehydration of the lapillus as it fell from the cloud into drier air, but it might have continued slowly as the lapillus lay on the ground surface.

What is the composition of the cement? It cannot be any mineral that is water soluble because it would not survive in porous lapilli in the rainy environment of the Isla Isabela. Therefore, chlorides, sulfates, and salts of K, Na and NH_4 can be eliminated from consideration. Carbonates cannot be the cement because the lapilli did not react in hydrochloric acid. Furthermore, EDS on fracture surfaces (non-carbon coated in a variable pressure SEM) did not show the presence of carbon so calcite is ruled out. Similarly, EDS on fracture surfaces did not show sulfur or chlorine (Section 4) so halite or gypsum/anhydrite are not likely cements. The absence

of chlorine may indicate that the water supplied during water–magma interaction and fragmentation had little or no sea water, or that chlorine was lost during palagonization or smectite formation.

Our investigations suggest that the lamellar coating is most likely composed of a variety of smectite resulting from crystallization of palagonite. High magnification SEM images show that the lamellar coating's morphology is virtually identical to that of smectite found in many other areas. Smectite has been directly linked to the temporal and chemical evolution of palagonite^{12-16, 24}, and its composition is consistent with our chemical analysis.

8. The role of water vapor in palagonization

There would appear to be two types of palagonization: subaquatic and aerial. The former takes place when hot lava meets liquid water, as on the sea floor. Aerial palagonization occurs when hot lithic clasts interact with water vapor in the atmosphere (including in eruption columns). The main difference between the two is the presence of air, i.e., gaseous nitrogen and oxygen. While subaquatic and aerial palagonization would appear to be distinctly different processes, perhaps they are not.

When water touches hot lava at low confining pressures, it instantly flashes into steam such that liquid water spends essentially no time in contact with the lava. The steam acts as a barrier between lava and liquid water, i.e., the Leidenfrost effect²³. Thus, subaquatic palagonization—until the lava cools to below about 100° C or thereabouts—occurs primarily between the lava and hot water vapor. Pressure in the deep ocean may prevent vaporization. Aerial palagonization also takes place between lava clasts and water vapor. Given enough water vapor in the eruption column, water vapor will always be in contact with the clasts. It therefore seems likely that both types of palagonization should be similar. Owing to palagonization's strong temperature dependence, either type would be expected to occur primarily at high temperatures.

If water vaporizes upon contact with hot lava, one might expect the vapor to form gas bubbles that rise from the contact area. Videos of pillow formation indeed show bubbles and a haze rising from the pillows. We think it likely that the haze is composed of microscopic water vapor bubbles. There probably is also a component of gas released by the lava.

The late stages of palagonization and eventual clay formation might also be similar. Once the lava cools

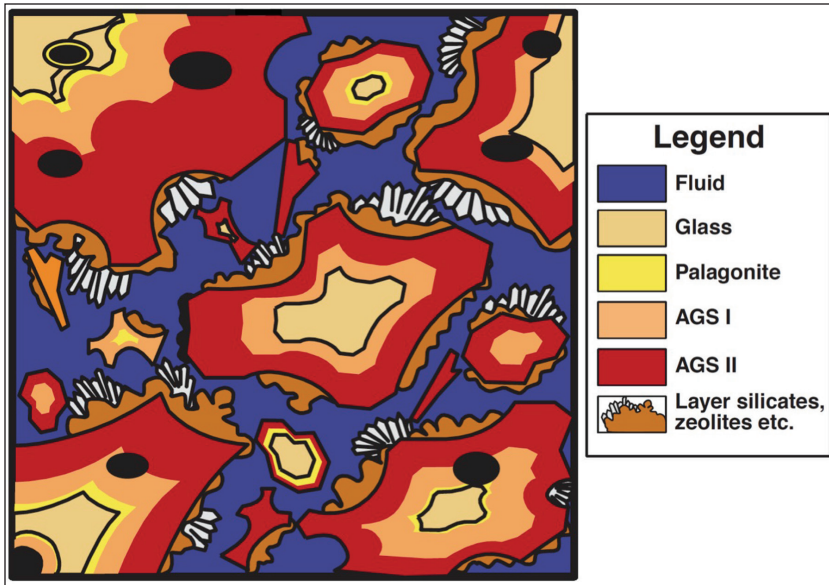


Figure 11. This drawing was taken from Figure 15 of Stronck and Schmincke²⁴. AGS I is mixed phase palagonite and crystals. AGS II is primarily crystalline. Note the overall similarity between their figure and our findings, specifically a glass clast surrounded by palagonite with “layer silicates, zeolites, etc.”, i.e., the same lamellar coatings we observe. While we agree with their layering of solids, we suggest that for the Tagus AL, much of the development of rinds on the glass takes place in the presence of water vapor, rather than “fluid”.

below 100° C, liquid water can remain in contact with it and palagonization will continue, though at a much slower rate. Since clay formation occurs after palagonization, it might happen more readily when liquid water is present. The same is true of aerial palagonization. Once the air temperature has dropped below 100° C (lower for higher elevations where the pressure is lower and the boiling temperature of water is depressed), liquid water will nucleate and water droplets will form. The water can interact with palagonite to continue the process of alteration, or it might promote formation of clay.

Most of the studies on palagonization are based on subaquatic conditions, while ours are unquestionably aerial in nature. Yet, our findings are quite similar to those from subaquatic palagonization and clay formation (Figure 11). Therefore a good case can be made for palagonization as a process mainly involving water vapor rather than liquid water.

9. Summary and conclusions

The main findings of this work are (1) the cement binding the Tagus cone AL together is a clay-like material, initially most likely palagonite and the thin layer of smectite and (2) the cement must have formed within a few minutes of the eruption. We further argue that subaquatic and aerial palagonite and clay formation

occur primarily in the presence of hot water vapor, with liquid water playing a smaller role.

The picture that emerges from our analyses suggest that the following steps took place sequentially to produce AL:

1. Vesiculating basaltic magma interacted with water (either seawater or groundwater) to form a phreatomagmatic eruption that propelled hot vitroclastic fragments into the air, where tiny glass shards congealed but remained much warmer than 100° C.

2. Palagonization began immediately upon exposure to hot water vapor, and a palagonite rind formed on every glassy clast.

3. Rinded clasts began colliding and sticking together, the earliest stage of accretory lapillus formation. The

presence of rinded clasts throughout the lapillus, and especially at its center, suggests that the rinds formed before or during aggregation. As the lapillus tumbled, it accumulated glass particles on every surface and became spheroidal. Concentric layering variations formed as the lapillus passed through different composition and particle size/concentration environments. The lapillus acquires an outer layer of much smaller closely packed clasts. The lapillus might have been only weakly bound together by touching palagonite rinds and bridges between grains.

4. Cement derived from crystallized palagonite and in the form of lamellar coatings (smectite) is developed on every surface. These crystals grew along the outer layers of palagonite, and where these layers from adjacent clasts connected, the cement interlocked and bound the AL together. At this point the spheroidal lapillus hardened. This hardening might have occurred while the lapilli were still suspended in the erupting column and/or plume, or during falling to the ground.

5. As the lapillus descended and cooled below water’s condensation temperature (less than or equal to 100° C depending on the altitude), water may have condensed within and onto the lapillus.

6. The fully indurated accretionary lapillus fell to the ground. Some dehydration of the palagonite and formation of smectite might have continued slowly as the lapillus lay on the ground surface, but there are no textural differences between these possible products and those formed during the aggradation and falling of the lapilli.

Any use of trade, firm, or product names is for descriptive purposes only and does not imply endorsement by the U.S. Government.

10. References

1. Moore, J.G. and Peck, D.L., 1962, Accretionary lapilli in volcanic rocks of the western continental United States; *The Journal of Geology*, Vol. 70, No. 2, p. 182–193.
2. Gilbert, J.S. and Lane, S.J., 1994, The origin of accretionary lapilli; *Bulletin of Volcanology*, v. 56, p. 398–411.
3. Schumacher, R., and Schmincke, H.-U., 1995, Models for the origin of accretionary lapilli; *Bulletin of Volcanology*, February, Volume 56, Issue 8, p. 626–639.
4. Brown, R.J., Branney, M.J., Maher, C., and Dávila-Harris, P., 2010, Origin of accretionary lapilli within ground-hugging density currents: Evidence from pyroclastic couplets on Tenerife; *Geological Society of America Bulletin*, v. 122 no. 1–2, p. 305–320. doi: 10.1130/B26449.1
5. Graup, Gunther, 1981, Terrestrial chondrules, glass spherules and accretionary lapilli from the suevite, Ries Crater, Germany; *Earth and Planetary Science Letters*, vol. 55, no. 3, p. 407–418.
6. Addison, W.D., Brumpton, G.R., Vallini, D.A., McNaughton, N.J., Davis, D.W., Kissin, S.A., Fralick, P.W. and Hammond, A.L., 2005, Discovery of distal ejecta from the 1850 Ma Sudbury impact event; *Geology*, v. 33, no. 3 p. 193–196.
7. Gánti, T., Pócs, T., Bérczi, Sz., Ditroi-Pukas, Z., Gal-Solymos, K., Horváth, A., Nagy, M., and Kubovics, I., 2005, Morphological investigations of martian spherules, comparisons to collected terrestrial counterparts; 36th Annual Lunar and Planetary Science Conference, March 14–18, 2005, in League City, Texas, abstract no. 2026.
8. Crowe, B.M. and Fisher, R.V., 1973, Sedimentary structures in base-surge deposits with special reference to cross-bedding, Ubehebe Craters, Death Valley, California; *Geological Society of America Bulletin*, v. 84, p. 663–682.
9. Wright, H.M., Mangan, M., Champion, D.E., Bindeman, I.N., and Vazquez, J.A., 2013, Explosive and effusive volcanism in the Salton Trough, Salton Buttes, CA; *American Geophysical Union, Fall Meeting 2013*, abstract #V13G-2701.
10. Brown, R.J., Bonadonna, C., and Durant, A.J., 2012, A review of volcanic ash aggregation; *Physics and Chemistry of the Earth*, v. 45–46, p. 65–78.
11. Rinard Hinga, B.D., 2015, “Ring of Fire: An Encyclopedia of the Pacific Rim’s Earthquakes, Tsunamis, and Volcanoes”; ABC-CLIO, Santa Barbara, p. 83.
12. Stroncik, N.A., and Schmincke, H.U., 2002, Palagonite - a review; *International Journal of Earth Science*, v. 91, p. 680–697.
13. Drief, A. and Schiffman, P., 2004, Very low temperature alteration of sideromelane in hyaloclastites and hyalotuffs from Kilauea and Mauna Kea volcanoes: Implications for the mechanism of palagonite formation; *Clays and Clay Minerals*, v. 52, no. 5, p. 623–635.
14. Berggaut, V., Singer, A., and Stahr, K., 1994, Palagonite reconsidered; paracrystalline illite-smectites from regoliths on basic pyroclastics; *Clays and Clay Minerals*, v. 42, p. 582–592.
15. Summers, K.V., 1976, The clay component of Columbia River palagonites; *American Mineralogist*, v. 61, p. 492–494.
16. Fisher, R.V. and Schmincke, H.-U., 1984, Alteration of volcanic glass; in “Pyroclastic rocks”, Springer, Berlin Heidelberg New York, p. 312–345.
17. Le Bas, M.J., Le Maitre, R.W., Streckeisen, A., and Zanettin, B., 1986, A chemical classification of volcanic rocks based on the total alkali-silica diagram; *Journal of Petrology*, v. 27, p. 745–750.
18. McPhie, J., Walker, G.P.L., and Christiansen, R.L., 1990, Phreatomagmatic and phreatic fall and surge deposits from explosions at Kilauea volcano, Hawaii, 1790 A.D.: Keanakakoi Ash Member; *Bulletin of Volcanology*, v. 52, p. 334–354.
19. Swanson D.A. and Christiansen, R.L., 1973, Tragic base surge in 1790 at Kilauea Volcano; *Geology* v. 1, p. 83–86.
20. Villermaux, E. and Bossa, B., 2009, Single-drop fragmentation determines size distribution of raindrops; *Nature Physics*, v. 5, p. 697–702.
21. Mueller, S.B., Kueppers, U., Ayris, P.M., Jacob, M., and Dingwell, D.B., 2016, Experimental volcanic ash aggregation: Internal structuring of accretionary lapilli and the role of liquid bonding; *Earth and Planetary Science Letters*, v. 433, p. 232–240.
22. Jakobsson, S.P. and Moore, J.G., 1986, Hydrothermal minerals and alteration rates at Surtsey volcano, Iceland; *Geological Society of America Bulletin*, v. 97, p. 648–659.
23. https://en.wikipedia.org/wiki/Leidenfrost_effect
24. Stroncik, N.A., and Schmincke, H.-U., 2001, Evolution of palagonite: Crystallization, chemical changes, and element budget; *Geochemistry, Geophysics and Geosystems*, v. 2, paper number 2000GC000102.